

## Moganite detection in silica rocks using Raman and infrared spectroscopy

PATRICK SCHMIDT<sup>1,\*</sup>, LUDOVIC BELLOT-GURLET<sup>2</sup>, VANESSA LÉA<sup>3</sup> and PHILIPPE SCIAU<sup>4</sup>

<sup>1</sup> Muséum National d'Histoire Naturelle, Dpt. de Préhistoire UMR 7194, Centre de Spectroscopie Infrarouge, CP 57, 57, rue Cuvier, 75231 Paris Cedex 05, France

\*Corresponding author, e-mail: schmidt@mnhn.fr

<sup>2</sup> Laboratoire de Dynamique, Interactions et Réactivité (LADIR) UMR 7075, CNRS and UPMC (Université Pierre et Marie Curie, Paris 6), 4 Place Jussieu, 75252 Paris Cedex 05, France

<sup>3</sup> TRACES — UMR 5608, Université Toulouse II le Mirail, Maison de la Recherche, 5, allée A. Machado, 31058 Toulouse Cedex 9, France

<sup>4</sup> CEMES, CNRS - UPR 8011 and Université de Toulouse, 29 rue Jeanne Marvig, 31055 Toulouse, France

**Abstract:** The quantitative determination of moganite in flint and chert plays an important role in the characterisation of these silica rocks and in the study of their genesis and evolution. Both Raman and infrared (IR) spectroscopy promise to be rapid and cost-effective tools for such studies. However, the use of vibrational spectra of moganite in silica rocks is hampered by the proximity of specific moganite bands with IR and Raman vibrations bands of non-bridging Si-O in silanol (SiOH) groups of chalcedony, the main coexisting silica phase. This may result in spectral interferences that lead to an overestimation of the moganite concentration. In order to calibrate quantitative moganite detection using IR and Raman spectroscopy, the spectra of chalcedony/moganite mixtures were studied using spectral decomposition. Heat treatment of the samples prior to their analysis is found to reduce the contribution of chalcedony silanol-bands to the measurement of the moganite bands, facilitating in this way the interpretation of the spectra. A new calibration curve is proposed for quantitative moganite detection using Raman spectroscopy. Infrared spectroscopy is also found to be useful for moganite quantification: a molar absorption coefficient of 43 L/mol·cm for the specific moganite-band at 575 cm<sup>-1</sup> is derived for the first time. The exact position of the specific IR and Raman moganite-bands is found to depend on whether the mineral occurs intermixed with chalcedony or in pure form. This study opens new prospects for quantitative moganite detection in silica rocks using vibrational spectroscopy.

**Key-words:** silica rocks, flint, chalcedony, chert, moganite, vibrational spectroscopy, silanol, spectral decomposition.

### Introduction

Commonly, sedimentary silica rocks are composed of micro-granular quartz and/or different types of chalcedony (Cayeux, 1929; Füchtbauer, 1988). Chalcedony is a spatial arrangement of 50–100 nm sized  $\alpha$ -quartz crystallites (Rios *et al.*, 2001). The crystallites align in fibres that can reach several millimetres or even centimetres in well crystallised specimens. In common silica rocks however, these fibres are usually shorter and somewhat less organised. Chalcedony mainly occurs in two forms, length-fast (LF) chalcedony with crystallites that have their *c*-axis oriented perpendicularly to the fibre axis and length-slow (LS) chalcedony with crystallites that have their *c*-axis oriented parallel to the fibre axis (Michel-Lévy & Munier-Chalmas, 1892). In both cases, numerous Brazil twin interfaces can be observed within the crystallites (Miehe *et al.*, 1984; Cady *et al.*, 1998) forming discontinuities and defect sites that allow the integration of chemically bound ‘water’ (Graetsch *et al.*, 1985). This silanol (SiOH) type adds to

the surface silanol that covers the surface of the crystallites and can represent up to 1 wt% of the rock (Flörke *et al.*, 1982).

Moganite is a silica polymorph commonly associated with chalcedony (Flörke *et al.*, 1976, 1984). Its structure can be described as a framework of (10 $\bar{1}$ 1) left- and right-handed quartz lamellae that alternate at the unit-cell scale, forming a monoclinic lattice (Miehe *et al.*, 1986; Miehe & Graetsch, 1992). The structure has therefore been associated with (10 $\bar{1}$ 1) Brazil-law twin boundaries in chalcedony (Miehe *et al.*, 1984). Apart from a phase transition between 296 °C and 316 °C (Heaney & Post, 2001; Heaney *et al.*, 2007), the thermal stability of moganite ranges up to 900–1000 °C where it transforms into cristobalite (Flörke *et al.*, 1984; Miehe & Graetsch, 1992). Moganite was identified in pure form only on Gran Canaria, Spain (Schmincke, 1969; Flörke *et al.*, 1976; Flörke *et al.*, 1984), where it occurs in fractures and voids within the ignimbrites of the Mogán Formation. Gran Canaria samples with lower moganite content are usually found in

association with LS-chalcedony in silica rocks that macroscopically resemble chalcedony. Besides this ‘classical’ occurrence, the mineral has been found in silica rocks all over the world, mainly intimately intergrown with both LS- and LF-chalcedony. Heaney & Post (1992) found moganite to be present in a large number of microcrystalline silica rocks where the mineral produces supplementary peaks in the powder X-ray diffraction pattern (Flörke *et al.*, 1984; Heaney & Post, 1992). A band in the moganite Raman spectrum near  $501\text{ cm}^{-1}$  was assigned to four-membered rings of  $\text{SiO}_4$  tetrahedra in the moganite structure (Kingma & Hemley, 1994; Heaney *et al.*, 2007). The spectra of chalcedony commonly show the well-known quartz bands and a supplementary band at a wavenumber close to one of the main moganite band. The ‘traditional’ interpretation of chalcedony Raman spectra was therefore that this band is caused by the moganite content of the samples (Rodgers & Cressey, 2001; Rodgers & Hampton, 2003; Nash & Hopkinson, 2004; Bustillo *et al.*, 2012). However, it was recently shown (Schmidt *et al.*, 2012) that the Raman band that is commonly observed in chalcedony is not uniquely caused by the moganite content of the analysed silica rocks. A band at  $503\text{ cm}^{-1}$ , resulting from non-bridging Si-O vibrations that are associated with the  $\approx 1\text{ wt\%}$  of chemically bound water forming silanol groups (SiOH), interferes with the main moganite-band. This overlap can make the Raman spectroscopic detection of moganite in the presence of silanol groups difficult. The infrared (IR) spectrum of moganite also shows a band that was described at frequencies ranging between  $565\text{ cm}^{-1}$  and  $572\text{ cm}^{-1}$  (Flörke *et al.*, 1976; Miede & Graetsch, 1992). Analogous to Raman spectroscopy, there is an infrared band caused by the vibration of non-bridging Si-O in silanol at  $555\text{ cm}^{-1}$  (Schmidt & Fröhlich, 2011), hence located close to the IR moganite absorption band.

Nevertheless, due to the characteristic moganite-bands, Raman and IR spectroscopy are rapid and cost effective means of moganite detection in silica rocks. Several quantitative studies using Raman spectroscopy have been published previously (Götze *et al.*, 1998; Rodgers & Hampton, 2003; Nash & Hopkinson, 2004; Bustillo *et al.*, 2012). However, most of these studies overestimated the moganite content of the studied samples because they took into account also the silanol-band during moganite quantification. The newest findings of the contribution of silanol to

the Raman signature of moganite (Schmidt *et al.*, 2012) create the need for a detailed re-evaluation of the feasibility of Raman quantitative studies for moganite detection. Infrared spectroscopy has been only very sporadically used for moganite detection in silica rocks but the problem of band interference is equally present in this technique. The moganite Raman and IR-absorption bands and their spectral environments are investigated here in detail. These two spectroscopic techniques are compared with classical quantitative determinations using X-ray powder diffraction data. Our study aims at creating a basis for quantitative determination of moganite in silica rocks by means of vibrational spectroscopy.

## Samples and experimental techniques

### Samples and sample preparation

Four samples from Gran Canaria (Spain) and France were used for IR and Raman analyses (Table 1). Moganite mostly occurs as translucent joint fillings in fractures of Gran Canaria ignimbrite of the Mogán formation (Flörke *et al.*, 1976; Flörke *et al.*, 1984). These silica veins are mostly pure moganite intermixed with LS-chalcedony. Commonly, at their exterior a white opaque rind shows higher moganite concentrations (Miede & Graetsch, 1992; Kingma & Hemley, 1994). Sample GC-11-06a is of this type. Mogán ignimbrites also contain nodular silica inclusions with the same composition; sample GC-11-16a is of this type. Both GC-11-06a and -16a show an identical micro-facies under the polarised-light microscope: short intersecting length-slow fibres. The third moganite sample, GC-11-01, is a compact whitish fracture infill with an opaque, almost powdery appearance (Fig. 1). This sample was found in a vertical fracture along with more consolidated material resembling that in GC-11-06a. The fourth sample, R-GE-Cal, is pure LF-chalcedony grown as a rim on a Cretaceous flint nodule from northern France with a moganite content of  $<1\%$  as determined by powder diffraction.

By the same means, GC-11-01 was found to be composed of moganite containing only halite (NaCl) as an impurity but no quartz. Halite was removed by repeated washing of the finely ground sample powder in deionised

Table 1. Samples and methods.

Sample Nr	Description	Analysis type
GC-11-01	White powdery joint filling material. Ignimbrite D, Mogán Formation. Gran Canaria, Spain. Miocene. Pure moganite with minor halite.	IR, Raman, XRD
GC-11-06a	Translucent joint filling material with white rind. Ignimbrite D, Mogán Formation. Gran Canaria, Spain. Miocene. LS-chalcedony and moganite.	Raman
GC-11-16a	Translucent nodular silicification. Ignimbrite D, Mogán Formation. Gran Canaria, Spain. Miocene. LS-chalcedony and moganite.	IR
R-GE-Cal	Botryoidal sedimentary LF chalcedony from a cavity in flint. From Upper Cretaceous chalk, Étretat beach, France.	IR, Raman, XRD

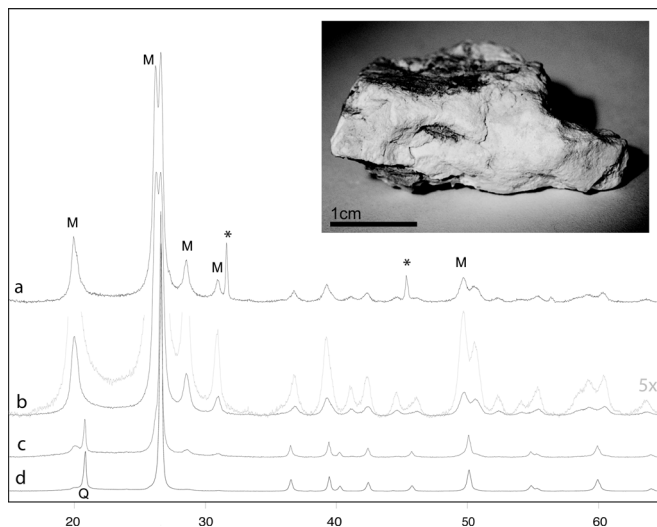


Fig. 1. X-ray powder diffractograms of moganite sample GC-11-01 before (a) and after washing/heat treatment (b) compared to reference sample powders with 50 wt% moganite (c) and 10 wt% moganite (d). Peaks that are exclusively assigned to quartz are labelled Q, moganite peaks M and halite peaks are labelled \*. Note that halite was completely removed from the moganite sample by washing and heat treatment. Mixed LF-chalcedony/moganite samples show strong quartz-peaks and weaker moganite-peaks. Inset: sample GC-11-01 before treatment.

water so that a highly pure moganite sample was obtained. In order to produce quantitative chalcedony/moganite calibration curves for IR and Raman spectroscopy, we selected samples R-GE-Cal and GC-11-01 as end-members. An earlier study (Schmidt *et al.*, 2012) showed that chemically bound hydroxyl in chalcedony may complicate the quantitative detection of moganite using vibrational spectroscopy. Silanol was therefore removed from the two powdered samples by means of heat treatment at 700 °C for 6 h. The resulting powders were then mixed at different ratios (in wt% moganite: 5, 10, 15, 20, 25, 30, 40, 50 and 75), using a balance with a precision of  $10^{-5}$  g. The powders of this set of reference samples, of 200 mg each, were homogenised by grinding in an agate mortar for 10 min before their use for moganite quantification.

### Instruments and settings

Raman spectra were acquired between  $100\text{ cm}^{-1}$  and  $1250\text{ cm}^{-1}$  using a Horiba Jobin Yvon HR800 spectrometer equipped with ultra narrow band Notch BraggGrate Filters for Rayleigh rejection. The exciting wavelength was the 514 nm line of an  $\text{Ar}^+$  laser that, in combination with a 2400 lines/mm grating, results in a spectral resolution of below  $0.4\text{ cm}^{-1}$ . The confocal hole which, in our setup also acts as a spectrometer entrance slit, was fixed at 300  $\mu\text{m}$ . Spectrometer calibration was set using the  $520.5\text{ cm}^{-1}$  band of a Si crystal. For the determination of precise band frequencies, the correct calibration of the spectrometer was verified before and after spectral acquisition. A 10x objective, producing an exciting spot of approximately 10  $\mu\text{m}$ ,

was used for spectral acquisition on powders and a 50x long working distance objective was used for spectral acquisition on unprepared bulk samples. Spectra were acquired during 1 min and 5 min for each spectral window (whole spectra from 4 min to 20 min in the case of 4 successive spectral windows).

Room temperature infrared transmission spectra were recorded between  $900\text{ cm}^{-1}$  and  $350\text{ cm}^{-1}$  using a Bruker VECTOR 22 spectrometer in direct transmission mode and unpolarised radiation. Spectral resolution was  $2\text{ cm}^{-1}$  and spectra were acquired using 200 scans for an optimal signal to noise ratio.

X-ray powder diffraction measurements were carried out on a Bruker D8 Advance device in Bragg Brentano geometry, equipped with a fast LynxEye detector and incident variable slits. Each powdered sample was inserted into a spinning sample holder in order to optimise measurement statistics. The X-ray wavelength used was that produced by a linear Cu anticathode. Diffractograms were acquired between  $15$  and  $90^\circ 2\theta$  with a step size of  $0.03^\circ 2\theta$  and a step time of 30 s. Rietveld quantitative phase analyses were performed using the Maud software (Lutterotti, 2010). Refined parameters were: phase scale factors, background coefficients, unit-cell parameters,  $z$ -shift error and peak-shape parameters. Structural parameters at room temperature were taken from Will *et al.* (1988) for  $\alpha$ -quartz and Heaney & Post (2001) for moganite, and not refined further.

### Experimental protocol and data treatment

#### Raman spectroscopy

Raman spectra were acquired on samples GC-11-01, GC-11-06a, R-GE-Cal and all mixed powders with reference moganite contents. Spectra of GC-11-01 were acquired on the bulk sample before any treatment and on a smeared mount of powder after washing and heat treatment. GC-11-06a was analysed at its central translucent part and at its outer white opaque rind with no prior preparation. Mixed powders with reference moganite contents were smeared on a glass slide and ten spectra were acquired at different spots on each flattened powder surface. These ten spectra were then averaged into one synthetic spectrum for further analysis. Error bars for the values obtained in this way are standard deviations calculated from the numerical dispersion of the values measured on the ten raw spectra before averaging. Raman intensities and band areas were obtained by fitting the spectra with Lorentzian functions.

#### Infrared spectroscopy

KBr pellets for IR transmission measurements were prepared from samples GC-11-01, GC-11-16a, R-GE-Cal and powders with 5 wt%, 10 wt%, 15 wt%, 20 wt%, 30 wt% and 50 wt% of moganite. All pellets were prepared from sample powders, the grain size of which was reduced to  $<2.5\text{ }\mu\text{m}$  by prolonged grinding (grain size was controlled with a microscope). An amount of  $2.5 \times 10^{-3}$  g of each sample was then mixed with 0.9975 g of KBr (balance

precision to  $10^{-5}$  g) and homogenised by grinding in an agate mortar for 5 min; 0.3 g of this mix were separated and pressed ( $1.1 \times 10^4$  kg/cm<sup>2</sup>) into a pellet. All infrared spectra underwent spectral decomposition in the spectral range between 620 cm<sup>-1</sup> and 360 cm<sup>-1</sup> for extracting parameters of the bands involved in the low-frequency absorption envelope. Lorentzian functions were used for the fitting of LF-chalcedony related bands, while moganite-bands were fitted with pseudo-Voigt functions in order to refine their band shapes. The molar absorption coefficient for the moganite-band at 575 cm<sup>-1</sup> was calculated from the slope of the regression line obtained from the measurements of powders with varying moganite content. A KBr density of 2.753 g/cm<sup>3</sup> and a molar weight of 60.08 g/mol for moganite were assumed for this calculation.

#### Powder-diffraction analysis

Samples GC-11-01, R-GE-Cal and mixtures with 10 wt%, 30 wt% and 50 wt% moganite were used for X-ray powder diffraction analysis and Rietveld refinement for the amounts of quartz and moganite. The obtained chalcedony/moganite concentration values served as reference measurements for the sample's composition.

## Results

### Moganite concentrations in the studied samples

Powder diffraction spectra of samples GC-11-01 and two mixed powders are shown in Fig. 1. Sample GC-11-01 is essentially pure moganite with no traces of quartz. Before treatment, the sample contained  $\approx 4$  % halite (Fig. 1a). After washing and heat treatment, no traces of halite were detected any more (Fig. 1b). Careful Rietveld refinement using the cell parameters of  $\alpha$ -quartz and moganite resulted in 99.99 % moganite and 0.01 % quartz. Oppositely, R-GE-Cal was found to be 99 % quartz and 1 % of moganite. The moganite and chalcedony contents in the mixed powders with different moganite concentrations, as determined by means of X-ray diffraction data, are summarised in Table 2. In all the cases, refinement of the diffractograms yielded quantitative results very close to the ratios used for preparing the powders. These results confirm the accuracy of moganite/chalcedony ratios of the mixed samples used for further analysis. They also illustrate that powder X-ray diffraction data in combination with appropriate data treatment is a very accurate tool for quantitative moganite detection in silica rocks.

### Raman spectroscopy

The Raman spectra of the pure moganite sample GC-11-01 before and after heat treatment/washing (Fig. 2c, d) are compared to the LF-chalcedony spectrum of R-GE-Cal (Fig. 2a, b). The spectra of GC-11-01 show no quartz-bands but all previously described moganite-bands (Kingma & Hemley, 1994). No difference in band position or relative intensity can be noticed between spectra acquired before and after treatment. The only discernable difference is that the bands of the heated powder are somewhat narrower than the ones in the untreated sample.

#### Position of the 500 cm<sup>-1</sup> moganite-band

The comparison between spectra acquired on two different areas on sample GC-11-06a, the white opaque outer rind and the translucent interior, reveals two main differences (Fig. 2e and f). First, the translucent interior part is composed of moganite intermixed with quartz (chalcedony) as it can be seen from the presence of a quartz-band at 464 cm<sup>-1</sup> whereas the white outer rind is pure moganite. The second difference is that the frequency of the main moganite-band shifts from 500 cm<sup>-1</sup> observed in the pure moganite rind to 501 cm<sup>-1</sup> observed in the chalcedony/moganite mixture. The band was also found at 500 cm<sup>-1</sup> in the pure moganite sample GC-11-01. This result indicates a band shift of 1 cm<sup>-1</sup> depending on whether moganite is pure or intergrown with quartz.

#### Quantitative moganite detection

As previously reported (Schmidt *et al.*, 2012), pure LF-chalcedony shows a silanol related band at 503 cm<sup>-1</sup> alongside its main quartz-band at 464 cm<sup>-1</sup>. After heat treatment, the 503 cm<sup>-1</sup> band disappears completely in spectra of the bulk sample (Fig. 2a) but grinding of the sample causes it to reappear (Fig. 2b). The reappearance is due to surface silanol groups that are created upon grinding. We used this fine quartz powder displaying the 503 cm<sup>-1</sup> band (Fig. 2b and top of Fig. 3a) for mixing with pure moganite powder at different ratios. During curve fitting of the 'mixed powder spectra', the band parameters of the 503 cm<sup>-1</sup> band (as determined in the pure R-GE-Cal powder spectrum) were set as fixed values in all spectra. In this way, the fit allows to precisely determine the band parameters of the moganite-band at 500 cm<sup>-1</sup> while the influence of surface silanol to the LF-chalcedony/moganite calibration curve is insignificant. Figure 3a shows Raman spectra of mixed powders with different moganite contents. It can be seen from the inset

Table 2. Chalcedony and moganite contents in mixed powders as determined by XRD and Rietveld refinement.

Ratio used for preparing the powders	Moganite detected by Rietveld refinement	Chalcedony detected by Rietveld refinement
10 wt% moganite	10.2 %	89.8 %
30 wt% moganite	30.3 %	69.7 %
50 wt% moganite	51.3 %	48.7 %



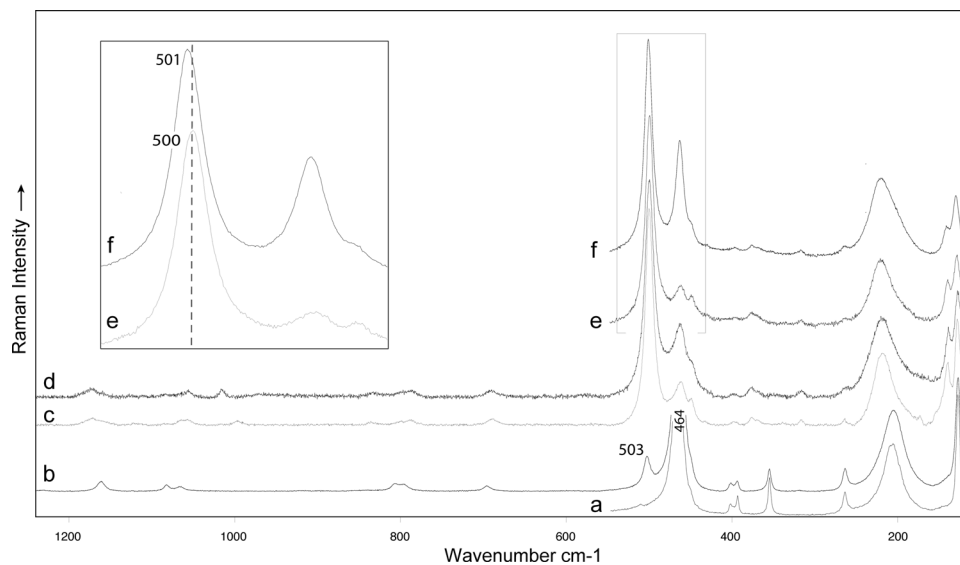


Fig. 2. Raman spectra of chalcedony and moganite samples. (a) Spectrum of LF-chalcedony sample R-GE-Cal after heat treatment but before grinding. Note the absence of a silanol-band at  $503\text{ cm}^{-1}$ . (b) Spectrum of the same sample R-GE-Cal after grinding. Grinding introduces new surface silanol shown by the appearance of a band at  $503\text{ cm}^{-1}$ . (c) Spectrum of moganite sample GC-11-01 after washing/heat treatment and (d) before any sample preparation. Note the narrower band shape after heat treatment allowing better discrimination of small bands. (e) Spectrum of the outer white rind of sample GC-11-06a. The spectrum shows no quartz-bands and identifies the white rind as pure moganite. (f) Spectrum of the inner translucent part of GC-11-06a identifying this part of the sample as moganite intermixed with quartz. The inset is an enlargement of spectra e and f in the zone marked by a rectangle. The position of the strongest moganite-band is  $500\text{ cm}^{-1}$  in pure moganite and  $501\text{ cm}^{-1}$  in the quartz/moganite mixture.

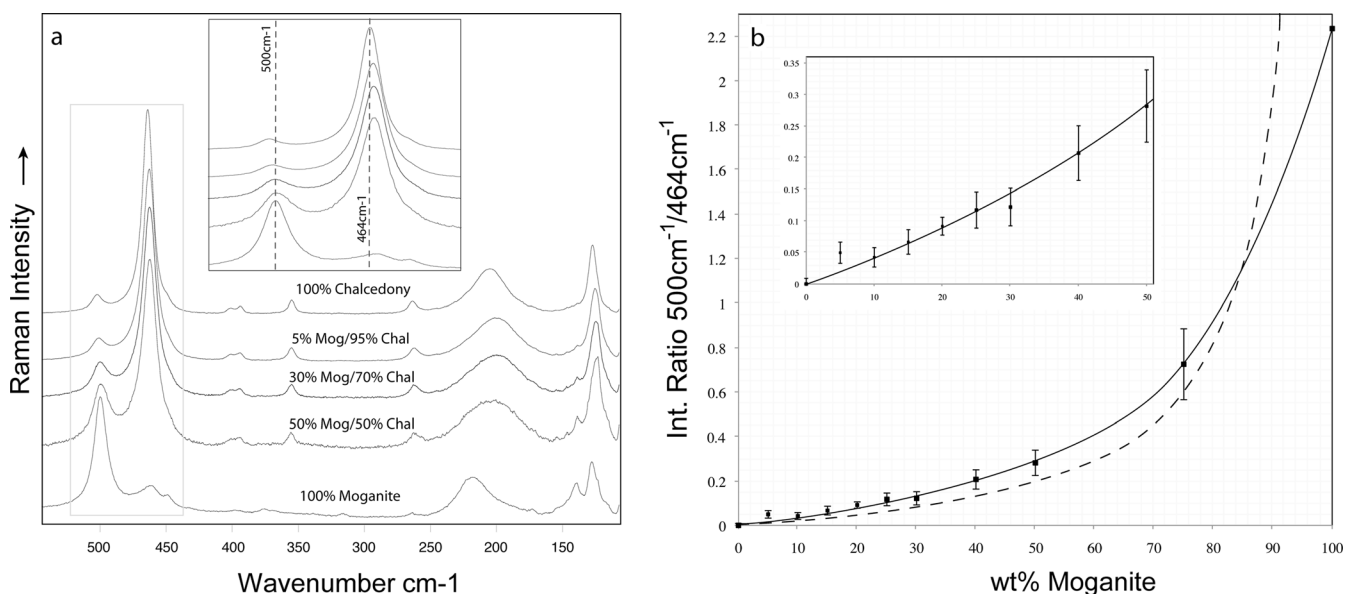


Fig. 3. (a) Raman spectra of powders with different LF-chalcedony/moganite ratios. The inset shows the enlargement of the spectral region marked by a rectangle. Note the shift in position of quartz- and moganite-bands as a function of the powders' moganite concentration. This shift is due to spectral interference of LF-chalcedony- and moganite-bands. (b) Calibration curve of the integral  $500/464\text{ cm}^{-1}$  band ratio obtained by the fitting of Raman spectra of LF-chalcedony/moganite powders (solid line). A similar curve published by a previous study (Götze *et al.*, 1998) is shown by the broken line for comparison. The inset shows the enlargement of the curve in the region of low moganite concentration.

that the band positions shift to lower wavenumbers with increasing moganite content. Careful curve fitting shows this shift to be due to interference between the  $503\text{ cm}^{-1}$  silanol-band and the  $500\text{ cm}^{-1}$  moganite-band. The same kind of interference can be noticed between the quartz

$464\text{ cm}^{-1}$  band and the two moganite-bands at  $463\text{ cm}^{-1}$  and  $449\text{ cm}^{-1}$ . Figure 3b shows the calibration curve obtained from fitting of the LF-chalcedony/moganite powder spectra. Plotted is the  $500/464\text{ cm}^{-1}$  integral ratio against the moganite content (in %). The curve has

a somewhat exponential shape implying that the determination of low moganite contents may be imprecise due to the weak slope of the curve in this region and the relatively large dispersion of the measurements.

## Infrared spectroscopy

### Quantitative moganite detection

Figure 4 shows the infrared spectra of heat-treated pure moganite (GC-11-01), LF-chalcedony (R-GE-Cal) and two intermediary LF-chalcedony/moganite mixtures (25/75 and 30/70, in %). Only the low-frequency envelope between  $650\text{ cm}^{-1}$  and  $350\text{ cm}^{-1}$  is different in the two silica polymorphs. Moganite- and quartz-bands can be identified by careful fitting of the absorption envelope: nevertheless their interference makes it difficult to precisely measure the corresponding band parameters. Only the moganite-band at  $575\text{ cm}^{-1}$  is sufficiently isolated to allow quantitative measurements. Analogous to Raman spectroscopy, the  $575\text{ cm}^{-1}$  IR-moganite-band interferes with a silanol-related chalcedony-band at  $555\text{ cm}^{-1}$  (Schmidt & Fröhlich, 2011). However, both bands are better individualised in the infrared spectra as compared to the Raman spectra. Thus, fitting the IR curve with fixed components allows the measurement of the band parameters (*i.e.*, one band fixed at  $575\text{ cm}^{-1}$  and another one at  $555\text{ cm}^{-1}$ ). Upon heat treatment, the  $555\text{ cm}^{-1}$  silanol-band is lost whereas heat treatment has no effect on the  $575\text{ cm}^{-1}$  moganite-band. Even though grinding introduces new surface silanols and, hence, the reappearance of a weak band at  $555\text{ cm}^{-1}$ , fitting of the spectra was found

to be greatly facilitated by heat treatment. It is also noteworthy that the  $575\text{ cm}^{-1}$  moganite-band shape was in all cases found to be a Gaussian function.

Chalcedony and moganite-bands used for the decomposition of the IR spectra are summarised in Table 3. The values plotted in Fig. 5 correspond to linear band intensities at  $575\text{ cm}^{-1}$  as obtained by these fits (all plotted values were obtained by fitting the spectra obtained from the analysis of the KBr pellets containing 0.75 mg of mixed powder each). The plot shows a linear regression of the absorbance as a function of the analysed moganite mass, proving in this way that the Beer-Lambert law can be used for quantitative moganite detection in chalcedony/moganite mixtures. The slope of the regression line allows one to calculate a molar absorption coefficient of  $43\text{ L/mol}\cdot\text{cm}$ .

### Position of the $575\text{ cm}^{-1}$ moganite-band

The moganite-band is not centred at precisely  $575\text{ cm}^{-1}$  in all the studied samples. Especially in those with lower moganite content, the band is shifted to lower wavenumbers. The fit of GC-11-16a, a sample with a moganite content of 26 % (as determined using the molar absorption coefficient of  $43\text{ L/mol}\cdot\text{cm}$ ), shows this band located at  $560\text{ cm}^{-1}$ . After heat treatment at  $700\text{ }^\circ\text{C}$  for 6 h, the band shifts to  $570\text{ cm}^{-1}$ . Figure 6 illustrates the fit of the band before and after heat treatment. It can be clearly seen that the exact band position is the result of the interference of the moganite-band and the chalcedony-silanol-band at  $555\text{ cm}^{-1}$ . Therefore, the resulting band shifts to higher wavenumbers when the silanol-band is lost. The same is to be expected for samples with different moganite concentrations, where

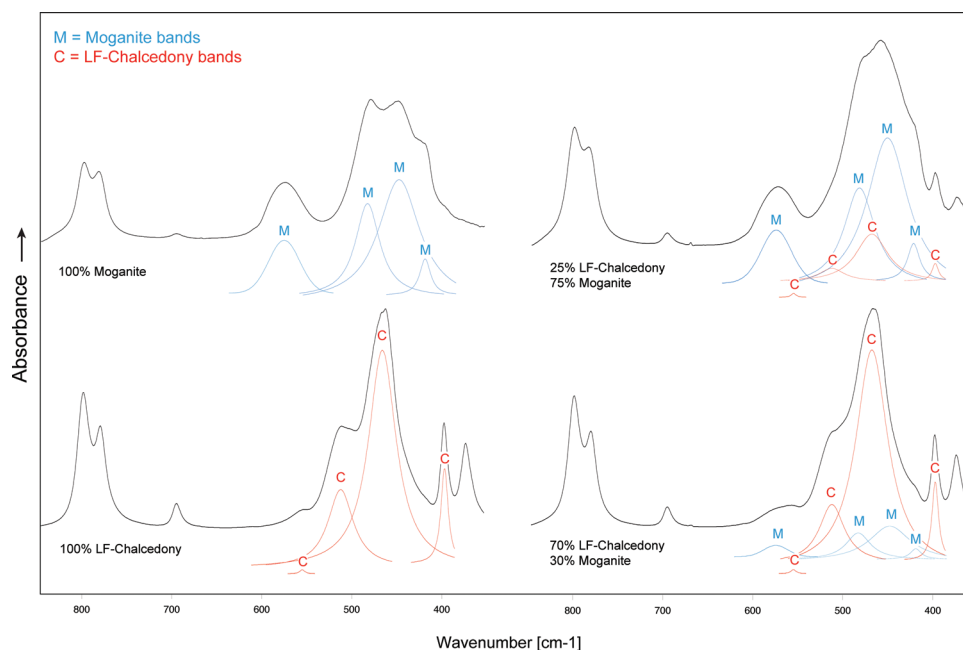


Fig. 4. Infrared spectra of LF-chalcedony sample R-GE-Cal, moganite sample GC-11-01 and two intermediary powders. Bands obtained by fitting the spectra are labelled C for LF-chalcedony-bands and M for moganite related bands. Positions of these bands are summarised in Table 2. Note the interference between the moganite-band at  $575\text{ cm}^{-1}$  and the LF-chalcedony silanol-band at  $555\text{ cm}^{-1}$  that can be best appreciated in spectrum 30% moganite/70%LF-chalcedony.

Table 3. Chalcedony- and moganite-bands used for decomposition of the IR spectra.

Band position [ $\text{cm}^{-1}$ ]	Assignment
373	Quartz
297	Quartz
420	Moganite
450	Moganite
464	Quartz
480	Moganite
513	Quartz
555	Quartz
575	Moganite

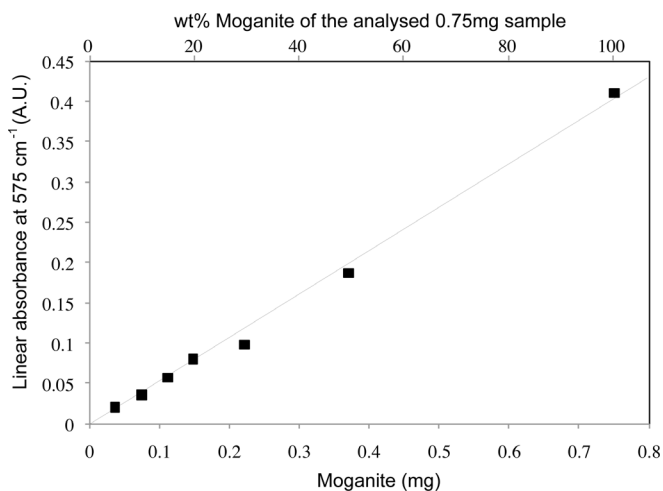


Fig. 5. Linear absorbance values of the moganite infrared band at  $575 \text{ cm}^{-1}$  as a function of the analysed mass of moganite. The best fit of the values results in a linear regression line showing the validity of the Beer-Lambert law for IR moganite quantification using this band. The linear absorbance values were obtained by fitting the IR spectra of powders with different LF-chalcedony/moganite ratios.

higher moganite concentrations induce a shift to higher wavenumbers of this characteristic band.

## Discussion

### Raman spectroscopy

The band position of the major moganite-band has been reported to be located at different wavenumbers. Most authors identified it at  $501 \text{ cm}^{-1}$  (Kingma & Hemley, 1994; Rodgers & Cressey, 2001; Nash & Hopkinson, 2004; Heaney *et al.*, 2007) but it was also identified at  $502 \text{ cm}^{-1}$  (Götze *et al.*, 1998; Bustillo *et al.*, 2012) and  $500 \text{ cm}^{-1}$  (Schmidt *et al.*, 2012). Although the precise measurement of Raman band positions depends on the resolution of the used spectrometer and its calibration, our results confirm that the location of this band may be also sample-specific. We prove that the position of the  $500 \text{ cm}^{-1}$

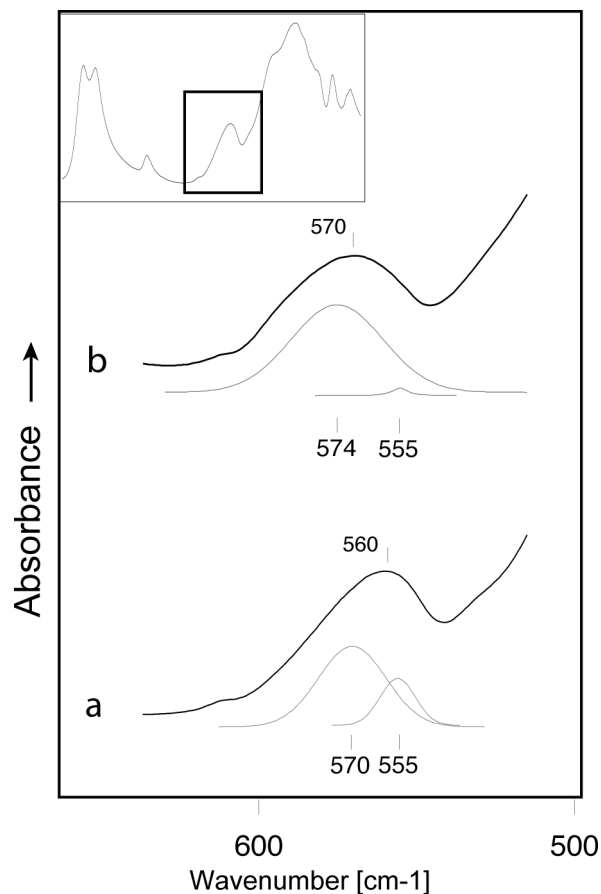


Fig. 6. Infrared spectra in the region of the specific moganite-band near  $570 \text{ cm}^{-1}$  in sample GC-11-16a before (a) and after heat treatment at  $700 \text{ }^\circ\text{C}$  (b). The band actually observed in the spectra is composed of two components, the LF-chalcedony silanol-band at  $555 \text{ cm}^{-1}$  and the moganite-band near  $570 \text{ cm}^{-1}$ . Upon heat treatment, the silanol-band is greatly reduced and the overall shape and position of this spectral region is modified.

moganite-band depends on whether the mineral is pure or intermixed with chalcedony. However, whether the shift from  $500 \text{ cm}^{-1}$ , observed in pure moganite, to  $501 \text{ cm}^{-1}$ , observed in mixtures, is due to interferences between a  $500 \text{ cm}^{-1}$  band and a  $503 \text{ cm}^{-1}$  silanol-band or the frequency of the moganite-band itself shifts because of interaction between phonons cannot be decided in this study.

The Raman spectra obtained during the analysis of mixed powders with different moganite contents highlight several bands that can be used for moganite detection in silica rocks. Candidates for this purpose are the intensity measurement of the moganite-band near  $140 \text{ cm}^{-1}$  and the fit of the soft mode near  $207 \text{ cm}^{-1}$  that is shifted to higher wavenumbers with increasing moganite content. However, the current spectra did not provide means for precise band-parameter determination of these weaker bands because of the relatively poor signal/noise ratio in the measurements on powders. The potential of these bands for moganite quantification is to be investigated in further studies. The best candidate for building a calibration curve was found to be the ratio between the major quartz- and moganite-bands, as already proposed by

earlier authors (Götze *et al.*, 1998). However, our calibration curve has a different shape from the previously published one (Fig. 3b). The difference may be related to two factors. When determining their calibration curve, Götze *et al.* (1998) did not take into account the contribution of the moganite-bands at  $463\text{ cm}^{-1}$  and  $449\text{ cm}^{-1}$ . The results were significantly higher  $501/464\text{ cm}^{-1}$  ratio values for high moganite concentrations. Another major difference is that the previously published curve was obtained from mixtures of moganite and macro-crystalline quartz. This produced lower ratio values in the region of low moganite concentrations as compared to our results. The reason is that the  $464\text{ cm}^{-1}$  band in quartz single crystals shows better Raman diffusion than the same band in LF-chalcedony, as the intensity of Raman diffusion is influenced by crystallinity. The new calibration curve proposed here can therefore be expected to be more precise for moganite content evaluation in LF-chalcedony/moganite mixtures, like flint or other micro-crystalline silica rocks. However, in general, the use of Raman spectroscopy for moganite quantification is not straightforward and requires a special protocol for sample preparation. It is difficult to evaluate with accuracy the contribution of silanol within the chalcedony fraction, thus results will most likely overestimate the moganite content of the samples. If, however, such a quantification is to be attempted, we recommend that the samples are heat-treated at minimum  $600\text{ °C}$  (but better at  $700\text{ °C}$  or  $800\text{ °C}$ ) for silanol ‘dehydration’. Also, it is of importance that multiple spectra are acquired on the bulk sample. Grinding should be avoided because it introduces new surface silanols, increasing in this way the silanol band at  $503\text{ cm}^{-1}$ .

### Infrared spectroscopy

The band position of the IR moganite-band near  $575\text{ cm}^{-1}$  was previously reported at different wavenumbers:  $565\text{ cm}^{-1}$  (Flörke *et al.*, 1976) or  $572\text{ cm}^{-1}$  (Miehe & Graetsch, 1992). Our results show the exact band position to be a function of the interference of two components: the  $575\text{ cm}^{-1}$  moganite-band and the  $555\text{ cm}^{-1}$  chalcedony silanol-band. The exact relation between band position, moganite content and silanol concentration remains to be investigated. Further studies should also attempt to clarify if there is a vibrational interaction between the moganite and quartz lattices that may influence the absorption frequency of the moganite-band in individual samples.

Our results prove the feasibility of moganite quantification in silica rocks by IR spectroscopy. The proposed molar absorption coefficient of  $43\text{ L/mol}\cdot\text{cm}$  should be a good basis for such quantitative studies. Samples should be heat-treated in order to reduce the contribution of the  $555\text{ cm}^{-1}$  silanol-band to the overall absorbance of the measured band near  $575\text{ cm}^{-1}$ . The band absorbance should also be determined by carefully fitting the whole low-frequency envelope with the quartz- and moganite-bands reported in Table 3.

### Conclusion

We found that Rietveld refinement of high-quality powder diffraction data is the most accurate technique for the quantification of moganite in silica rocks like flint and chert. We also found that vibrational spectroscopy can be used for moganite quantification having the generic advantage of faster data acquisition. However, spectroscopic analyses aiming at quantitative moganite detection have to be performed very cautiously. The contribution of silanol-bands to the measurements should either be evaluated by carefully fitting the spectra or, better, silanols should be removed from the samples before the measurement. For Raman spectroscopic analyses, the samples should be heat-treated in order to ‘dehydrate’ hydroxyl, reducing the contribution of the Raman silanol signal to the Raman moganite signal. Grinding should be avoided prior to Raman analysis to prevent introducing new surface silanols. We also found infrared spectroscopy to be a valid tool for quantitative moganite detection that has some advantages over Raman spectroscopy: the validity of the Beer-Lambert law and therefore the possibility of direct quantitative measurements; better sample homogenisation and therefore more representative values for a whole sample. In infrared spectra, both moganite- and silanol-bands are better separated so that the fitting procedure is less ambiguous. However, for a good precision of the moganite quantification, samples should also be heat-treated and spectra should be carefully fitted using a model based on the moganite and quartz-bands reported in this work. Several questions concerning moganite-band positions and their relation to purity and spectral interference remain to be addressed by further studies.

**Acknowledgements:** We thank Nicolas Ratel-Ramond from CEMES, Toulouse, for technical support during X-ray diffraction measurements and Rietveld quantitative phase analysis. We also thank one anonymous reviewer for his/her constructive comments that led to improvement of the manuscript. Fieldwork at Gran Canaria, Spain, was funded by the ANR-09-BLAN-0324-01 ProMiTraSil research programme.

### References

- Bustillo, M.A., Pérez-Jiménez, J.L., Alonso-Zarza, A.M., Furio, M. (2012): Moganite in the Chalcedony Varieties of Continental Cherts (Miocene, Madrid Basin, Spain). *Spectrosc. Lett.*, **45**, 109–113.
- Cady, S.L., Wenk, H.R., Sintubin, M. (1998): Microfibrous quartz varieties: characterization by quantitative X-ray texture analysis and transmission electron microscopy. *Contrib. Mineral. Petrol.*, **130**, 320–335.
- Cayeux, L. (1929): Les Roches sédimentaires de France, Roches siliceuses. Impr. Nat, Paris, 774 p.



- Flörke, O.W., Jones, J.B., Schmincke, H.U. (1976): A new microcrystalline silica from Gran Canaria. *Zeit. Krist.*, **143**, 156–165.
- Flörke, O.W., Köhler-Herbertz, B., Langer, K., Tönges, I. (1982): Water in microcrystalline quartz of volcanic origin: agates. *Contrib. Mineral. Petrol.*, **80**, 324–333.
- Flörke, O.W., Flörke, U., Giese, U. (1984): Moganite, a new microcrystalline silica-mineral. *N. Jb. Mineral. Abh.*, **149**, 325–336.
- Füchtbauer, H. (1988): Sedimente und Sedimentgesteine. Schweizerbart, Stuttgart, 1141 p.
- Götze, J., Nasdala, L., Kleeberg, R., Wenzel, M. (1998): Occurrence and distribution of “moganite” in agate/chalcedony: a combined micro-Raman, Rietveld, and cathodoluminescence study. *Contrib. Mineral. Petrol.*, **133**, 96–105.
- Graetsch, H., Flörke, O.W., Mieke, G. (1985): The nature of water in chalcedony and opal-C from Brazilian agate geodes. *Phys. Chem. Minerals*, **12**, 300–306.
- Heaney, P.J., Post, J.E. (1992): The Widespread Distribution of a Novel Silica Polymorph in Microcrystalline Quartz Varieties. *Science*, **255**, 441–443.
- , — (2001): Evidence for an *I2/a* to *Imab* phase transition in the silica polymorph moganite at  $\sim 570$  K. *Am. Mineral.*, **86**, 1358–1366.
- Heaney, P.J., McKeown, D.A., Post, J.E. (2007): Anomalous behavior at the *I2/a* to *Imab* phase transition in SiO<sub>2</sub>-moganite: an analysis using hard-mode Raman spectroscopy. *Am. Mineral.*, **92**, 631–639.
- Kingma, K.J., Hemley, R.J. (1994): Raman spectroscopic study of microcrystalline silica. *Am. Mineral.*, **79**, 269–273.
- Lutterotti, L. (2010): Total pattern fitting for the combined size–strain–stress–texture determination in thin film diffraction. *Nucl. Instrum. Meth. B*, **268**, 334–340.
- Michel-Lévy, A., Munier-Chalmas, C.P.E. (1892): Mémoire sur les diverses formes affectées par le réseau élémentaire du quartz. *Bull. Soc. Fr. Mineral.*, **15**, 159–195.
- Mieke, G., Graetsch, H. (1992): Crystal structure of moganite: a new structure type of silica. *Eur. J. Mineral.*, **4**, 693–706.
- Mieke, G., Graetsch, H., Flörke, O.W. (1984): Crystal structure and growth fabric of length-fast chalcedony. *Phys. Chem. Minerals*, **10**, 197–199.
- Mieke, G., Flörke, O.W., Graetsch, H. (1986): Moganit: Strukturvorschlag für ein neues mikrokristallines SiO<sub>2</sub>-Mineral. *Fortschr. Mineral.*, **64**, 117.
- Nash, D.J., Hopkinson, L. (2004): A reconnaissance laser Raman and Fourier transform infrared survey of silcretes from the Kalahari Desert, Botswana. *Earth Surf. Proc. Land*, **29**, 1541–1558.
- Rios, S., Salje, E.K.H., Redfern, S.A.T. (2001): Nanoquartz vs. macroquartz: a study of the  $\alpha$  -  $\beta$  phase transition. *Eur. Phys. J. B*, **20**, 75–83.
- Rodgers, K.A., Cressey, G. (2001): The occurrence, detection and significance of moganite (SiO<sub>2</sub>) among some silica sinters. *Mineral. Mag.*, **65**, 157–167.
- Rodgers, K.A., Hampton, W.A. (2003): Laser Raman identification of silica phases comprising microtextural components of sinters. *Mineral. Mag.*, **67**, 1–13.
- Schmidt, P., Fröhlich, F. (2011): Temperature dependent crystallographic transformations in chalcedony, SiO<sub>2</sub>, assessed in mid infrared spectroscopy. *Spectrochim. Acta A*, **78**, 1476–1481.
- Schmidt, P., Bellot-Gurlet, L., Slodczyk, A., Fröhlich, F. (2012): A hitherto unrecognised band in the Raman spectra of silica rocks: influence of hydroxylated Si–O bonds (silanole) on the Raman moganite band in chalcedony and flint (SiO<sub>2</sub>). *Phys. Chem. Minerals*, **39**, 455–464.
- Schmincke, H. (1969): Ignimbrite sequence on Gran Canaria. *Bull. Volcanol.*, **33**, 1199–1219.
- Will, G., Bellotto, M., Parrish, W., Hart, M. (1988): Crystal structures of quartz and magnesium germanate by profile analysis of synchrotron-radiation high-resolution powder data. *J. Appl. Crystallogr.*, **21**, 182–191.

Received 14 September 2012

Modified version received 20 November 2012

Accepted 7 December 2012